Faculty of Electrical Engineering
Universiti Teknologi Malaysia

VOL. 9, NO. 2, 2007, 66-72

ELEKTRIKA
http://fke.utm.my/elektrika

Modeling of Sodium Sulfur Battery for Power System Applications

Zahrul F. Hussien[1*], **Lee W. Cheung**[1], **Mohd F. M. Siam**[2] and **Amir B. Ismail**[1]

[1]Power Engineering Centre, Universiti Tenaga Nasional, 43009 Kajang, Selangor, Malaysia.
[2]TNB Research Sdn Bhd, 43000 Kajang, Selangor, Malaysia.

[*]Corresponding author: zahrul@uniten.edu.my (Zahrul F. Hussien), Tel: 603-89287229, Fax: 603-89212116

Abstract: Sodium sulfur battery is an advanced secondary battery that is relatively new in power system applications. This paper presents the modeling and simulation of sodium sulfur battery used in power system applications such as for battery energy storage system and power quality custom devices. Several electrical battery models are reviewed and important factors to be considered in modeling the battery such as internal resistance, temperature effect, electromotive force and depth of discharge are discussed. Based on the available empirical data, the voltage-current behavior and characteristics of NAS battery are modeled in PSCAD/EMTDC software tool. The model is then used in simulation studies of power system applications utilizing NAS batteries.

Keywords: Battery energy storage system, Electrical battery model, NAS battery, Sodium sulfur battery.

1. INTRODUCTION

Battery energy storage is being used for various power system applications such as for load leveling, uninterruptible power supply and power quality custom devices. Sodium sulfur (NAS) battery is an advanced secondary battery developed by Tokyo Electric Power Company (TEPCO) and NGK Insulators, Ltd. since 1983 [1]. Feasibility studies of various demonstration projects showed that the NAS battery technology is attractive for use in relatively large scale battery energy storage system applications due to its outstanding energy density, efficiency, zero maintenance and long life cycle of up to 15 years [1-4]. Recent advances include the development of NAS battery for multiple function storage system that performs a variety of energy management function and custom power devices for power quality applications. The performance of NAS battery is the main factor in determining its effectiveness in these various applications, therefore the need for an accurate model is indispensable.

The objective of this paper is to propose an electrical model of a NAS battery that takes into account the various important factors such as energy, power, voltage, internal resistance, service life, depth of discharge and temperature as they influence the capacity, operational characteristics and performance of the battery. The validated proposed model could then be used in simulation studies of power system applications utilizing NAS batteries.

2. FEATURES OF NAS BATTERY

A schematic diagram of a NAS cell is shown in Figure 1. The cylindrical structure NAS cell uses sodium as the negative active material, sulfur as the positive active material and a solid beta alumina ceramics act as electrolyte by transferring sodium ions between the positive and negative electrodes. The metal container, which is housed inside the beta alumina tube, acts as a safety tube to prevent an over current and an internal temperature rise in case of a beta alumina tube failure. Table 1 shows specifications of a NAS cell.

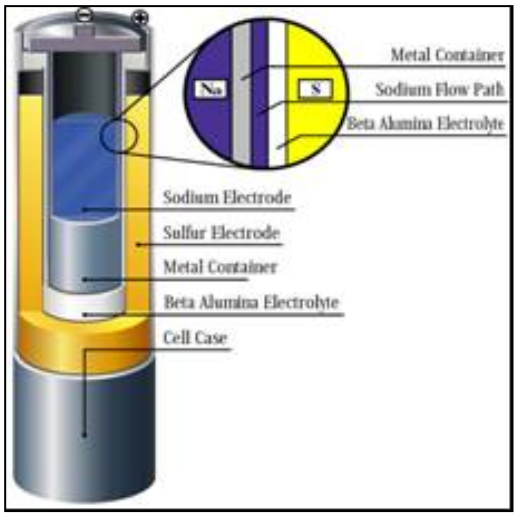

Figure 1. Schematic diagram of NAS cell structure

Table 1. Specification of NAS cell

Voltage	2 V
Capacity	1220 Wh
Dimensions	Diameter: 91 mm Length: 516 mm
Efficiency	89% (8-hour rate)
Energy Density	367 Wh/l
Weight	5.5 kg

NAS battery is usually used in the form of a battery module in which cells are collected and housed in a thermal enclosure as shown in Figure 2. The battery module is equipped with an electrical heater to raise and maintain cell temperature as NAS battery operates at an optimal temperature of nearly 300° C. Cells inside the module are anchored in place by filling and solidifying them with sand to prevent fires. Table 2 shows the specifications of a NAS battery module. The features and advantages of NAS battery are discussed in detail in [1, 2, 7, 8].

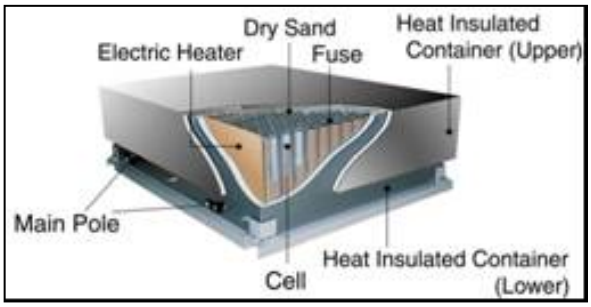

Figure 2. 50kW NAS battery module structure

Table 2. Specification of NAS battery module

Power Output	52.1 kW
Voltage	58 V/116 V
Current	726 A/363 A
Capacity	375 kWh
Efficiency	>83%
Dimensions	W:2.17 m; D:1.69 m; H:0.64 m
Weight	3.5 ton
Energy Density	160 kWh/m^3
No. of Cells	320

In this work, the model of a single NAS cell is first developed and validated. Then, the model is extended to represent a NAS battery module since the NAS battery is usually used in this form where a number of NAS cells are connected together to give higher power and energy capacity.

3. IMPORTANT FACTORS IN NAS BATTERY MODELLING

In order to model the NAS battery accurately, the factors discussed in the following sections such as the internal resistance, service life, temperature, electromotive force and depth of discharge are vital to determine battery capacity and voltage-current behavior.

3.1 Internal Resistance

The internal resistance of the NAS battery consists of the ohmic resistance associated with electrolyte resistance, plate resistance and fluid resistance, and the resistance associated with the polarization effect. The internal resistance varies during charging and discharging operation depending upon the depth of discharge and temperature as demonstrated in Figure 3. The figure consists of two groups of curves, one for the charging operation and the other is for the discharging operation at five different cell temperatures. The curves show how the internal resistance varies with the depth of discharge for different cell temperature. It can be observed that the internal resistance reduces as temperature increases from 280° C to 360° C. Also observed at the end of charging and discharging operation is the polarization effect that tends to increase the internal resistance. These ranges of depth of discharge have to be avoided in the operation of the NAS battery due to the excessive increase in internal resistance.

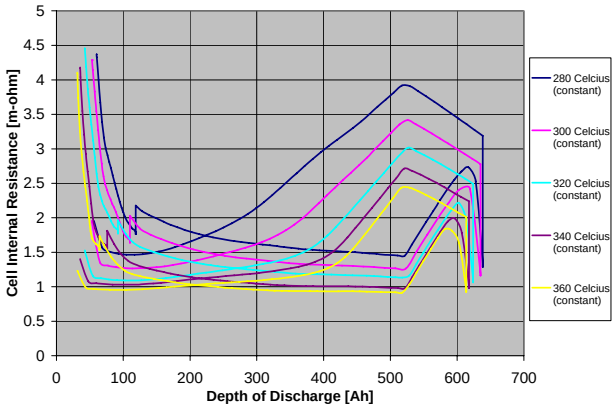

Figure 3. Depth of discharge vs. internal cell resistance at different temperature (Experimental)

The internal resistance also varies due to the life cycle resistance that depends upon the number of the charge-discharge cycle already experience by the battery. As demonstrated in Figure 4, the internal resistance increases as the number of charge-discharge cycle increases. This factor is important as it determines the remaining available maximum pulse power and voltage output of a NAS battery.

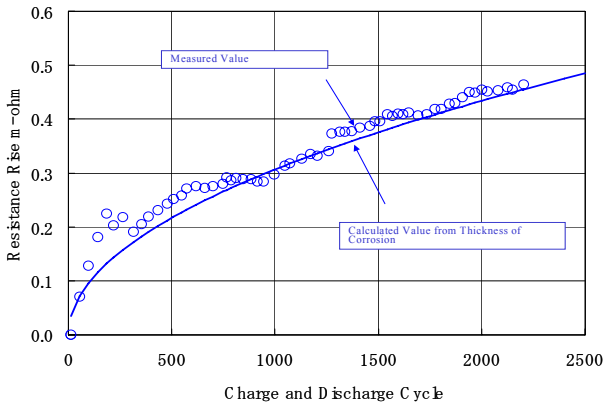

Figure 4. Cell-deterioration resistance vs. charge-discharge cycle (Manufacturer Data)

3.2 Temperature Effect

NAS battery operates around 300-360° C. Its temperature varies differently between charging, standby and discharging state of operation. During discharging state, NAS battery generates resistance heat and entropic heat causing the battery to store heat and raises its temperature. While at charging state, the amount of resistance heat generation is nearly equal to that of

entropic heat absorption. Thus, the battery temperature is gradually lowered. Heat stored in the battery only dissipated during standby state. As a result, the battery temperature drops gradually. When the temperature exceeds the lower limit (300° C), the heater installed inside the BM will be turned on to raise the temperature and maintain it within nominal temperature range. The NAS battery resistance varies with the temperature where the higher the module temperature, the smaller the internal resistance become.

The effect of temperature on the internal resistance is very important as it determines the limit to the battery's peak power output. In some applications, NAS batteries are subjected to pulse output of up to 4-5 times the rated power output [1, 2, 7]. Pulse power output with larger current generates more joule heat by internal resistance. For example, a 50 kW NAS battery module with 5 times rated power output for 30 seconds will make temperature rise by around 3° C [7]. During these pulse power operations, the temperature must be kept within normal operating condition in order to avoid reaching unacceptably high temperature and creating undesirable temperature differentials within the battery.

3.3 Battery Electromotive Force

The electromotive force (EMF) of NAS battery depends mainly on the depth of discharge. Due to the composition reaction, the EMF of NAS battery is relatively constant but drops linearly after 60-75% depth of discharge as shown in Figure 5.

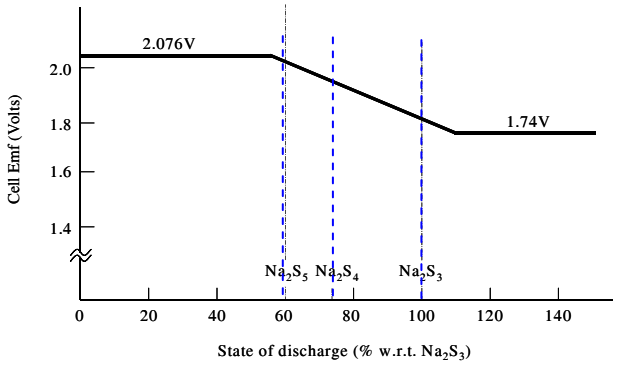

Figure 5. NAS cell electromotive force vs. depth of discharge

In practice, NAS battery is limited to discharge to less than 100% of its theoretical capacity because of the more corrosive properties of Na_2S_3. Before all the materials change to Na_2S_3, the sodium in the cell move to active electrode and the room for sodium becomes empty. In such a case, there is no path for electron in the negative electrode, causing poor performance at discharging. Hence, the battery is designed to stop discharging before all the sodium goes to active electrode. To provide an operational safety margin, the remaining volume of sodium per cell has to be considered. For example in a total sodium volume of 780 g, the usable sodium is 675 g that make the remaining volume of sodium to be 13.5%.

As a result, NAS cell typically deliver 85-90% of their theoretical capacity which means the approximate sodium polysulfide composition corresponding to 1.82 V per cell is a mixture of Na_2S_4 and Na_2S_2 at the end of discharge. This factor is important and needs to be considered in the simulation in order to observe the voltage level at the end of discharge and to predict the possible maximum power output of the NAS battery at any depth of discharge.

3.4 Depth of Discharge

Depth of discharge (DOD) represents the capacity left in the battery. It is important as it is related to the internal resistance change, temperature and battery's EMF level.

4. NAS BATTERY MODELS

In this section, several battery models are reviewed and described for modeling the NAS battery characteristic. Subsequently, one of these is selected to be most suitable to model and represent most of the important behavior of the NAS battery.

4.1 Simple Model

The most commonly used battery model is shown in Figure 6, consisting of a constant internal resistance (*Ro*) and open circuit voltage (*Eo*) where *Vo* is the terminal voltage of the battery [5]. Since NAS battery's internal resistance is sensitive to and varies with temperature and depth of discharge, this model is not suitable in modeling the battery because it does not take into account the varying characteristic of the internal resistance of the battery with respect to depth of discharge and temperature changes. The simple model can only be applied in simplified case studies where the energy from Eo is assumed to be unlimited.

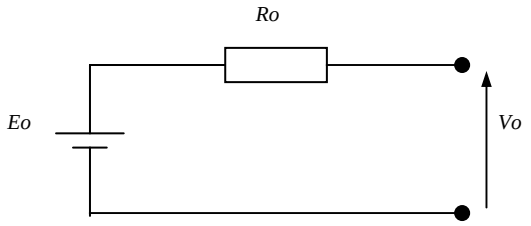

Figure 6. Simple battery model

4.2 Thevenin Battery Model

The second most commonly used is the Thevenin battery model, which includes an ideal no load battery voltage (*Eo*), internal resistance (*R*), capacitance (*Co*) and over-voltage resistance (*Ro*) as shown in Figure 7 [5,6].

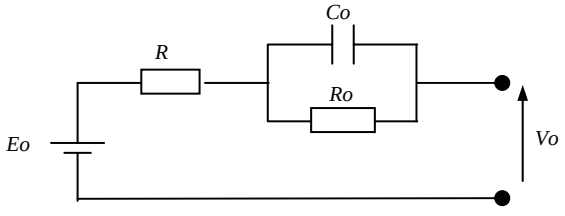

Figure 7. Thevenin battery model

In modeling the NAS battery, the disadvantage of this model is that the elements are assumed to be constant, whereas in actuality all the elements values are related to

battery conditions [5]. In addition, the internal open circuit voltage drop (EMF drop) in NAS battery is not taken into account.

4.3 Modified Battery Model

This battery model as illustrated in Figure 8 is relatively simple but yet meets most requirements for modeling the NAS battery.

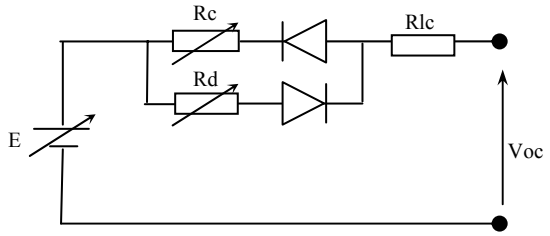

Figure 8. Modified battery model

It is a modified battery model based on the basic configuration of the simple battery model. It takes into account the non-linear battery element characteristic during charging and discharging as well as the internal resistance which depends on the temperature changes and depth of discharge of the battery previously discussed in section 3. Therefore, it is selected as the most appropriate in modeling the NAS battery using EMTDC/PSCAD simulation tool. Based on the NAS battery characteristic, the components in the modified battery model are described as follows.

4.3.1 Charge and Discharge Resistances, Rc and Rd

Rc and Rd internal resistance are a function of the temperature and depth of discharge. The purpose of the diodes is to make NAS battery possessing different internal resistance value during charge and discharge operation.

4.3.2 Charge-Discharge Lifecycle Resistance, Rlc

Rlc represents deterioration-resistance that is based on the number of charge-discharge life cycle resistance.

4.3.3 Battery Open-Circuit Voltage, E

E represents the cell's EMF as a function of depth of discharge. Based on the characteristic shown in Figure 5, it is expressed as follows:

$$E = Eo \quad ; \text{at DOD} \leq 60\ \%$$
$$E = Eo - k.f \quad ; \text{at DOD} > 60\ \%$$

where k is a constant obtained by experiment, f is the depth of discharge (%) and Eo is EMF at fully charged.

The modified battery model of Figure 8 represents the performance of one NAS cell. A battery energy storage system uses battery modules which includes several cells connected in series and/or parallel. In this work, a 50 kW NAS battery module (Type G50), which consists of 320 cells connected in series for high capacity storage device is selected. The voltage-current behavior of the 50 kW battery module can be estimated and simulated by multiplying the internal cell resistance and cell's EMF by 320 based on the given internal cell resistance data and performance information from battery manufacturer.

4.4 Simulation Model in PSCAD/EMTDC

The modeling and simulation of the NAS battery is carried out using PSCAD/EMTDC, an industry standard simulation tool for studying the transient behavior of electrical networks. Using one of the built-in components available in PSCAD, the important manufacturer data and parameters are tabulated and compiled into a data-reference look-up table. Consequently, the feature of components Rc, Rd, E and Rlc are plotted and derived from the data-reference look-up table by using linear interpolation or extrapolation depending on the input value of depth of discharge and temperature.

Figure 9(a) shows the PSCAD component used, the XYZ component which outputs the value of z (Rd curve) based on the input values x (temperature-change) and y (Depth of discharge, %) using interpolation by referring to the references files based on the experimental data.

Detail of this XYZ relationship is illustrated in Figure 9(b) where the values of internal cell resistance for different depth of discharge and temperature are plotted.

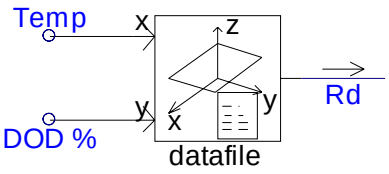

(a)

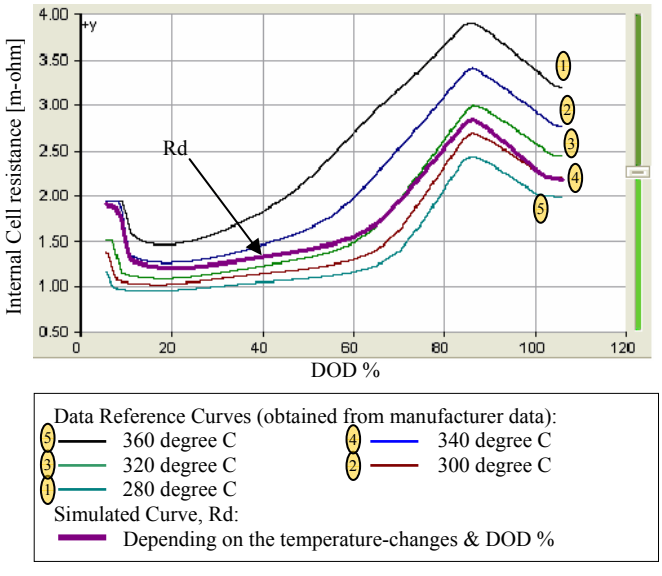

(b)

Figure 9 (a) XYZ Component provided in PSCAD (b) Simulated Rd-curve as a function of temperature and DOD%.

5. SIMULATION RESULTS AND VALIDATION

The simulation is divided into two parts. First, the electrical NAS battery model is tested and simulated as per cell basis to examine its voltage-current behavior at

different power output discharge level. Then, the model is modified to simulate the pulse power capability of 50 kW battery module (320 cells in series). Both simulation results are compared with the experimental results for validation.

5.1 NAS Cell Simulation Results

In order to validate the NAS cell electrical battery model, simulation is carried out and its result is compared with the experimental result for peak shaving application as follows:

- 4 hours of constant power discharging at 84 W
- 3 hours of constant power discharging at 136 W
- 4 hours of constant power discharging at 84 W
- 2 hours standby
- 9 hours of constant power charging at 135 W

Figures 10 and 11 present the results obtained from the simulation and experiment respectively. Generally, the characteristic and behavior of the NAS cell terminal voltage and current obtained from experimental measurement agree well with the simulation.

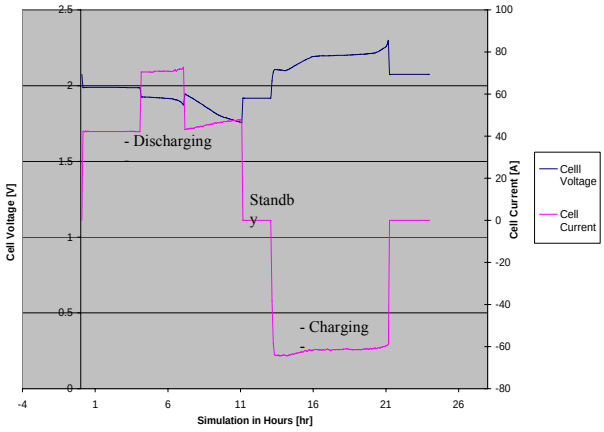

Figure 10. Voltage-current behaviour of a NAS cell (Simulation)

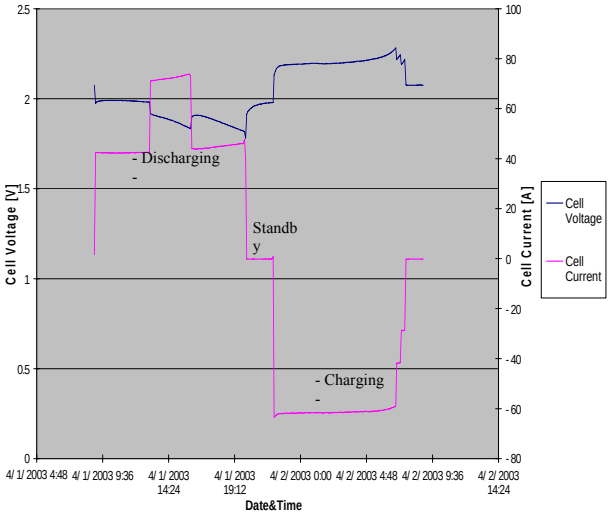

Figure 11. Voltage-current behaviour of a NAS cell (Experimental)

It has to be noted that upon closer inspection, the simulated terminal voltage waveform shown in Figure 10 is observed to differ slightly from that in Figure 11 at several instances which can be explained as follows.

The simulation does not take into account the short duration alteration of polarization effect at the edge of switching operation which slightly affects NAS internal resistance in practice. However, this polarization effect is known to be of little concern in peak shaving application hence it is not taken into consideration in the simulation studies [2].

Also, the pattern at the end of charging is different between simulation and experimental. In practice, the internal resistance rises at the end of charging operation as shown earlier in Figure 3 due to the insulating nature of pure sulfur [8]. If NAS battery continues to be charged at constant power, its internal resistance increases significantly causing larger energy loss at higher terminal voltage. To avoid this, when terminal voltage reaches a set point, charging power is decreased to reduce excessive energy loss. This process is called "supplement charge" as is evidently shown in Figure 11. However, the "supplement charge" process is not taken into account in the simulation model for simplicity. The cell is only subjected to a constant charging power, which raises the terminal voltage as it comes to the end of charging.

Lastly, it can be seen that the behavior of voltage and current demonstrated a concave pattern at the shoulder discharging hours on both simulation and experimental results. During discharging, the EMF of NAS battery decreases when depth of discharge exceeds around 60%. Hence, the cell is pushed to produce higher output current for a constant power output with the drop in terminal voltage.

5.2 50kW NAS Battery Module Simulation Results

After the validation of the NAS cell model, a 50 kW NAS battery module is then simulated to perform peak shaving operation for 5 hours duration at 50 kW, combined with a series of 30 s pulse power events for PQ applications at approximately 250 kW (5 times the rated power). The pulse power events are scheduled at 1 hour intervals between each pulse. The initial temperature of the battery is set at 295° C.

Figure 12 shows the variation in the temperature and the output power of the battery module throughout the duration of the simulation. It can be clearly seen that the battery module temperature increases at a steady rate of about 7° C during the 50 kW discharging operation. During each pulse power event that lasted for 30 s each, the temperature increases more rapidly by about 3° C. In practice, the allowable upper limit of the battery module temperature is set at 360° C. Inspection of the output power reveals that the pulse power output will be lower at the starting and at the end of discharge e.g. first pulse power output is lower than the second one, the fifth pulse power output is lower than the fourth one. This is due to the higher internal resistance at the starting and at the end of discharge (as exhibited by the experimental result in Figure 3).

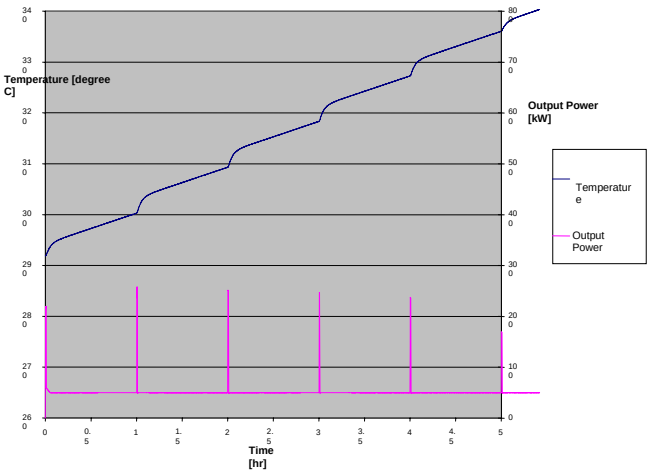

Figure 12. Temperature change in a 50kW NAS battery module during operation (Simulation)

6. APPLICATION EXAMPLE

As an example application of the NAS battery model, a line-interactive standby power system (SPS) for the mitigation of voltage sags and peak shaving has been studied in simulation software EMTDC/PSCAD. A block diagram of the standby power system topology is shown in Figure 13.

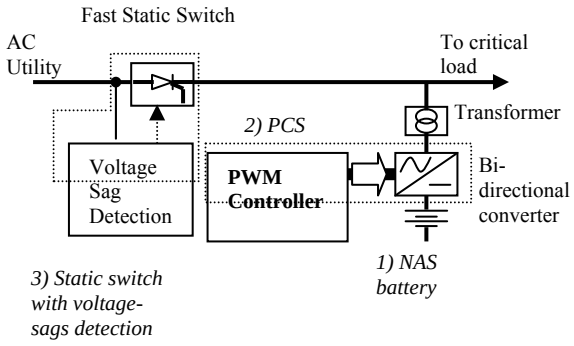

Figure 13. Schematic diagram of line-interactive standby power supply

This topology consists of three main parts; battery storage, power conversion system and static switch with voltage-sags detection. During normal condition, the battery is charged by operating the converter in rectification mode and the load is supplied directly from utility via static switch. For PQ operation when interruption or voltage-sags occurs, the fast static transfer switch will open in about half a cycle time and the power flows from battery to the load through the converter, which is operated in inverter mode.

The inverter output should be synchronized to the line voltage in order to provide smooth transfer from utility source to the battery and minimal amount of disturbance is seen by the load. The SPS could also function in peak shaving mode while simultaneously protecting the critical load from voltage-sags. During the daytime peak hours, the battery is discharged at constant rated power and the power flow from the battery via converter (inverter mode) to the load for shaving the peak demand.

The studied system consists of two NAS battery module, which are connected in parallel having 100 kW for peak shaving application and 400 kW for PQ application. A critical load of 400 kW is connected to the 415 V bus. The load is supplied by the utility when a single-phase fault is applied at one of the phase for duration of 0.5 s. The magnitude of the single phase voltage sag is approximately 30%. The following simulations were carried out to assess the effectiveness of the proposed NAS electrical battery model in voltage-sag mitigation:

Case 1: The NAS SPS not in operation

Case 2: The NAS SPS in operation

Figure 14 and Figure 15 show the load voltage and the power flow for Case 1 and Case 2 respectively. In Case 1, the single phase fault causes the voltage to sag during the duration of the fault. In Case 2, when the fault is detected by the voltage sag detector, a logic signal is send to the static switch in order to isolate the load from the faulted supply. From this instance, the load is fully supplied by the NAS battery. The SPS system takes about half a cycle (10 ms) for the static switch to open and NAS standby power supply to restore the voltage.

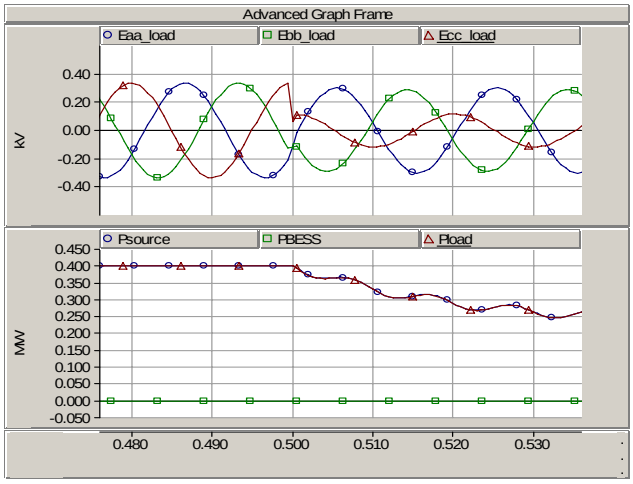

Figure 14. Load voltage and power flow without NAS line-interactive standby power supply (Case 1)

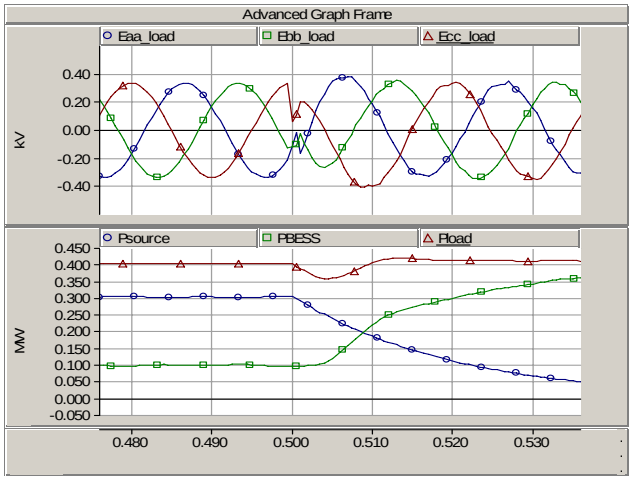

Figure 15. Load voltage and power flow with NAS line-interactive standby power supply (Case 2)

7. CONCLUSION

This paper presented an electrical battery model of NAS battery that can be used in simulation studies of the battery in power system applications. Important factors such as energy, power, voltage, internal resistance, service life, depth of discharge and temperature are taken into account in the battery model. The comparisons between simulation and experimental results have proven that the battery model is accurately simulating the NAS battery. Example application in the performance simulation study of line interactive standby power supply using NAS battery is presented. It highlighted the use of the developed NAS battery model in a simulation study whose purpose is to examine the capability of NAS battery in mitigating voltage sag.

ACKNOWLEDGEMENT

This work was jointly supported by Tokyo Electric Power Company (TEPCO), TNB Research Sdn. Bhd. and University Tenaga Nasional.

REFERENCES

[1] M. Kamibayashi and K. Tanaka, "Recent Sodium Sulfur Battery Applications," *Proc. IEEE PES Transmission and Distribution Conference and Exposition*, USA, 2001, Vol.2, 28 Oct.-2 Nov. 2001, pp. 1169-1173.

[2] B. Tamyurek, D. K. Nichols and O. Demirci, "The NAS Battery: A Multi-Function Energy Storage System," *Proc. IEEE PES General Meeting*, USA, 2003, Vol. 4, 13-17 July 2003.

[3] F. M. Stackpool, W. Auxer, M. McNamee and M. F. Mangan, "Sodium Sulphur Battery Development," *Proc. 24th Intersociety Energy Conversion Engineering Conference*, 1989, IECEC-89, Volume 6, August 06-11, 1989, pp 2765 – 2768.

[4] K. Takashima, F. Ishimaru, A. Kunimoto, H. Kagawa, K. Matsui, E. Nomura, Y. Matsumaru, A. Kita, S. Iijima, T. Kato, Y. Matsuo, T. Nakayama, Y. Sera, "A Plan for a 1MW/8MWH Sodium-Sulfur Battery Energy Storage Plant," *Proc. 25th Intersociety Energy Conversion Engineering Conference*, 1990. IECEC-90., Vol. 3, August 12-17, 1990, pp 367 – 371.

[5] H.L. Chan and D. Sutanto, "A New Battery Model for use with Battery Energy Storage System and Electrical Vehicles Power Systems," *Proc. IEEE PES Winter Meeting 2000*, Vol. 1, Jan. 23-27, 2000, pp 470-475.

[6] Yoon-Ho Kim and Hoi-Doo Ha, "Design of Interface Circuits With Electrical Batter Models," *IEEE Transactions on Industrial Electronics*, vol.44, No.1, February 1997.

[7] H. Takami, A. B. Ismail and M. F. M. Siam, "NAS Battery Energy Storage System for Power Quality Support in Malaysia," *Proc. International Power & Energy Conference*, IPEC2003 Conf., November 28, 2003.

[8] D. Linden and T. Reddy, "Handbook of Batteries," Third Edition, McGraw-Hill, 2002, pp 40.1-40.23.